PERGAMON

Atmospheric Environment 33 (1999) 2031–2043

ATMOSPHERIC ENVIRONMENT

Buoyant plume rise described by a Lagrangian turbulence model

Stefan Heinz[a,*], Han van Dop[b]

[a] *Department of Applied Physics, Delft University of Technology, Thermal and Fluid Sciences, Lorentzweg 1, 2628 CJ Delft, Netherlands*
[b] *Institute for Marine and Atmospheric Research (IMAU), Utrecht University, P.O. Box 80.005, 3508 TA Utrecht, Princetonplein 5, Netherlands*

Received 8 July 1998; accepted 3 November 1998

Abstract

A Lagrangian turbulence model is presented, which describes buoyant turbulence fully consistent with Eulerian budget equations as motion of fluid particles and change of their temperatures. This model is applied to the description of buoyant plume rise. Due to the simulation the turbulent mixing processes between the plume and ambient fluid in dependence on varying ambient conditions, the plume rise model presented here offers different advantages in comparison to existing models: the different plume rise phases are calculated consistently and the full plume statistics is obtained. The model predictions are compared to consequences of the similarity theory, results of large-eddy simulations and lidar measurements of the plume height and width in the atmosphere. For different flows with varying shear and stratification, we find in all these comparisons a good agreement between our computations and measurements, simulations and theoretical predictions. In particular, it is shown that the similarity theory appears as a special case of the theory presented here. The simplicity and the low computational costs of our model make it well-suited for routine applications.

Keywords: Turbulent dispersion; Buoyancy; Lagrangian stochastic models; Turbulence models; Similarity theory

1. Introduction

Prediction of buoyant plume rise is a standard problem in environmental research that has been considered since decades with more and more advanced simulation techniques, as, e.g. by Csanady (1973), Briggs (1975), Zannetti and Al-Madani (1984), Cogan (1985), Nieuwstadt and de Valk (1987), Weil (1988), Netterville (1990), van Dop (1992), Nieuwstadt (1992a, b), Luhar and Britter (1992), Anfossi et al. (1993), Hurley and Physick (1993), Zhang and Ghoniem (1993, 1994a, b), Erbrink (1994), Gangoiti et al. (1997) and Weil et al. (1997). One reason for this interest is the direct practical relevance of this problem, e.g. for the assessment of the dispersion of stack plumes. Their temperature is usually higher than that of the environment, and such temperature differences may have a drastic influence on the spatial distribution of emitted substances and, in particular, their ground concentrations. A second reason for the continuous research interest in buoyant plume rise is of theoretical nature, because this problem represents a standard case for simulations of the turbulent mixing of fluids with different temperatures. The complexity of such mixing processes is illustrated in Fig. 1, where the turbulent mixing of a buoyant stack plume and the ambient air is shown. In

* Corresponding author. Tel.: +31 15 278 3649; fax: +31 15 278 1204; e-mail: heinz@wt.tn.tudelft.nl.

1352-2310/99/$ - see front matter
PII: S1352-2310(98)00414-2

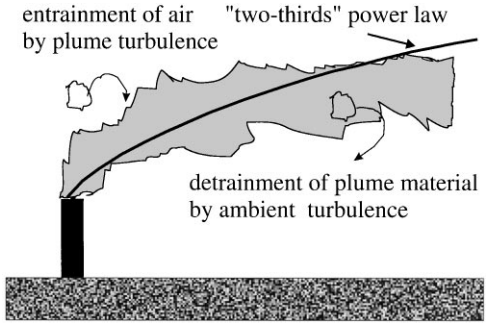

Fig. 1. Illustration of the turbulent mixing between a buoyant (stack) plume and the ambient flow.

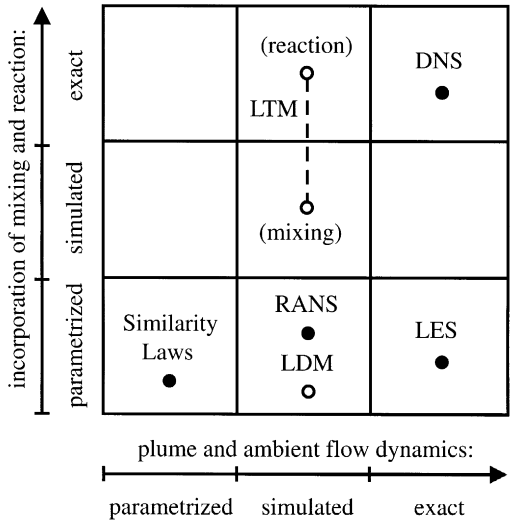

Fig. 2. Illustration of differences of various techniques with respect to the calculation buoyant plume rise. As acronyms are used: Reynolds-averaged Navier–Stokes (RANS) methods, large-eddy simulation (LES), direct numerical simulation (DNS), Lagrangian dispersion models (LDM) and Lagrangian turbulence models (LTM). The solid circles denote Eulerian methods and open circles denote Lagrangian methods.

the initial stage, the turbulent mixing is dominated by the entrainment of air into the plume by the plume-generated turbulence. This process leads to the observed "two-thirds" power law for the mean plume rise (Csanady, 1973; Briggs, 1975) that is shown in Fig. 1. Detrainment, i.e. entrainment of plume material into the surrounding fluid due to ambient turbulence (Netterville, 1990), may then take place at later times. This process leads to deviations from the two-thirds power law: the plume levels off, where the final plume height is determined by shear and stratification of the ambient flow.

Different methods for the explanation of buoyant plume rise are compared to each other in Fig. 2. As criteria, we consider the parametrization, simulation and exact description of the dynamics of the plume and the ambient flow, where the treatment of the turbulent mixing between them (and for completeness the treatment of chemical reactions between species that may be distributed in the plume and the surrounding flow) is characterized by the same criterias. Similarity theory provides parametrizations for the mean plume height and width (Csanady, 1973; Briggs, 1975) if the influence of the ambient turbulence can be neglected, i.e. if the turbulence is generated only by the plume. This applies to the initial stage of plume rise, and for emissions into neutrally stratified ambient flows with a negligible turbulence. Under these conditions one finds the two-thirds power law for the mean plume height. Combined with empirical modifications that take the influence of stratification into account, these plume rise formulas may often be applied as guidelines for the assessment of practical problems, as described, for instance, by Weil (1988), Erbrink (1994) and Gangoiti et al. (1997). The problem of these approaches is related to the fact that such fittings to measurements have limited ranges of applicability and cannot provide predictions for conditions where measurements are hardly available or not of sufficient accuracy. Just this is often found to be the case for plume rise measurements in the atmosphere under complex conditions, as for instance in respect to the assessment of shear effects (Djurfors and Netterville, 1978; Weil, 1988).

For practical plume rise calculations, models are required that (i) are computationally not too expensive, (ii) can be applied to both stages of the buoyant plume rise and different ambient conditions, and (iii) permit the assessment of fluctuations, i.e. provide also plume statistics. The attempt to derive directly such models leads within the Eulerian framework to Reynolds-averaged Navier–Stokes (RANS) equations, and within the Lagrangian framework to Lagrangian dispersion models (LDM), see Fig. 2. RANS equation methods (Weil, 1988; Netterville, 1990; Gangoiti et al., 1997) apply parametrizations for terms that are related to the turbulent mixing of the plume and the ambient flow (and chemical reactions if reactive plumes have to be calculated). A shortcoming of RANS techniques is that they have to introduce parameters that cannot derived directly from measurements, such as a "turbulence buffet frequency" (Netterville, 1990; Gangoiti et al., 1997) that reflects the influence of ambient turbulence. Additionally, previously applied methods only provide the averages of plume characteristics, which are used then for the assessment of statistical variations. By means of Lagrangian methods both the mean plume behaviour and the plume statistics can be described in accord with constraints of the similarity theory and observations. This was demonstrated by van Dop (1992) in a first systematic analysis of the description of buoyant plume rise by Lagrangian methods. Alternative methods are described by Anfossi

et al. (1993), where a review can be found on earlier work (see Zannetti and Al-Madani, 1984; Cogan, 1985) to describe buoyant plume rise by means of Lagrangian methods, and for convective conditions by Luhar and Britter (1992), Hurley and Physick (1993) and Weil et al. (1997). Such Lagrangian dispersion models (LDM) simulate the plume dynamics, but they require knowledge about the flow field that has to be provided by Eulerian models or approximated. Entrainment and detrainment are reflected in LDM by parametrizations of time scales. These concepts lead to questions, if variations of mixing processes, e.g. due to shear and stratification, have to be described.

Lagrangian turbulence models (LTM) extend LDM to the whole fluid (Heinz, 1997, 1998a), this means they describe the motion and properties of plume-particles and fluid particles that represent the ambient flow, see Fig. 1. In particular, these Lagrangian equations are constructed so that usual Eulerian budget equations are fully satisfied, see Section 2. This concept overcomes the problems of RANS equations and LDM that are described above (Heinz, 1998b). In contrast to LDM, LTM calculates simultaneously the plume and the ambient flow and, in particular, their turbulent mixing in dependence on shear and stratification. In contrast to RANS equation methods, LTM provides the plume statistics and avoids the introduction of parameters that cannot be measured. Apart from these differences to RANS equations and LDM, the great advantage of LTM is that arbitrary complicated nonlinear chemical reactions can be treated without having to make additional assumptions (Pope, 1985). In analogy to direct numerical simulation (DNS), LTM resolves mixing and chemical reaction processes for high-Reynolds number flows, see Fig. 2. The main difference between DNS and LTM is that the high computational costs of DNS make this method only for flows with low Reynolds and Damköhler numbers realizable, whereas LTM can be applied to arbitrary flows due to its much lower computational costs. This fact is of considerable practical relevance, because only a few turbulent flows of engineering and environmental interest are characterized by low Reynolds and Damköhler numbers. In respect to practical applications, LTM also offers advantages compared to large-eddy simulation (LES) that applies approximations only for the smallest scales (Nieuwstadt and de Valk, 1987; Nieuwstadt, 1992a, b; Zhang and Ghoniem, 1993, 1994a, b), see Fig. 2. The reason for that are twofold: first, the computational effort of LES and its current limitation to simple geometries makes it less attractive for routine applications, and second, the derivation of simple (integral) models for buoyant plume rise from LES which would be applicable for regulatory applications is difficult (Nieuwstadt and de Valk, 1987; Nieuwstadt, 1992a, b). In contrast to this, the latter can be achieved by simplifying LTM, as demonstrated here.

The main concern of this paper is to derive a buoyant plume rise model from LTM, which can be used for regulatory applications and satisfies the constraints (i)–(iii) considered above. The LTM is presented in Section 2, where the derivation of the Lagrangian equations and time scales that appear in these equations is described. In Section 3, a buoyant plume rise model is derived from LTM. In Section 4, the predictions of this model are compared to the consequences of similarity theory for a neutrally stratified flow and LES data for plume rise in a stably stratified flow. In Section 5, we compare our model predictions with results of plume rise measurement in the atmosphere. Finally, conclusions are drawn with respect to theoretical questions and practical applications.

2. Lagrangian turbulence models

The description of the motion of all fluid particles of the flow (i.e., of plume- and ambient-air particles, see Fig. 1) requires Lagrangian equations that are consistent with the Navier–Stokes equations. Two methods are used to date which are aimed at this consistency: first, the derivation of stochastic Lagrangian equations that are in consistency with RANS equations up to second order (van Dop et al., 1985; Sawford, 1986; Pope, 1994a; Heinz, 1997, 1998a), and second, the derivation of these equations in agreement with the one-point Eulerian velocity probability density function (PDF) (Thomson, 1987). Reviews of theoretical aspects of these developments can be found in Sawford (1993), Pope (1994b) and Rodean (1996), and the progress in the solution of practical questions (in particular by means of the second approach) was described by Wilson and Sawford (1996).

The second approach requires the joint velocity–temperature PDF, which poses a complicated problem for the conditions considered here. In contrast to convective boundary layer turbulence, e.g. this PDF cannot be considered as a simple superposition of modes that reflect the upward and downward motions, but it has a more complex structure resulting from modes that reflect the upward buoyant-motion and the damping influence of the ambient turbulence. Therefore, the first approach is applied here. This method requires closure assumptions for the pressure redistribution and dissipation terms in the RANS equations of second order that are used to construct the Lagrangian models, see Section 2.2. Such parametrizations are known and relatively well-investigated for buoyancy-affected flows (see, e.g. Craft et al., 1996).

It is worth emphasizing that Lagrangian models derived in that way differ considerably from (second-order) RANS equations, although they are constructed in consistency with them: First, such LTM enable a much more comprehensive description of turbulence, because not only the dynamics of some moments of the joint velocity-

temperature PDF is described, but the PDF itself. This additional knowledge permits valuable insight, e.g. into flow structures (Heinz, 1998b) or, with regard to reacting flows, into the competition between mixing and reaction (Gonzales, 1997). Moreover, different closure problems of RANS equations do not appear, as those related to triple correlations or mean chemical conversion rates. Second, the applied consistency constraint does not affect the description of time scale variations, which is a central ingredient of turbulence models. It is accepted that many problems in RANS methods are related to such equations for the dissipation rate of turbulent kinetic energy (TKE), characteristic turbulence frequency or dissipation time scale. The difference between LTM and RANS equations with respect to this problem is given by the fact that instantaneous events (the mixing of momentum and scalar particle properties) are described in LTM. This means, that assumptions on the elementary mechanisms of mixing processes can be applied in LTM, whereas the effect of these processes on the dynamics of averaged (or filtered) quantities has to be predicted in RANS methods (or LES), which is obviously much more complicated.

In Section 2.1, the Lagrangian equations are introduced and the Eulerian transport equations for mean quantities and variances are derived from these equations. In Section 2.2, the coefficients in these equations will be evaluated, so that given second-order budget equations of turbulence are fully satisfied. More details about the derivation of stochastic Lagrangian equations for buoyant turbulence can be found elsewhere (Heinz, 1997, 1998a). In Section 2.3, the estimation of time scales is considered, which appear in the Lagrangian equations.

2.1. Lagrangian equations

PDF transport equations appear often as high-dimensional partial differential equations. An extremely fruitful way to look at such equations uses a Lagrangian representation following a fluid particle (Pope, 1994b; Thomson, 1987), because this approach makes a powerful numerical method available for their solution: Monte Carlo simulation (Fox, 1996). In such Lagrangian PDF methods, realizations of the PDF are described by stochastic differential equations (see, e.g., Gardiner, 1983; Risken, 1984). By restricting the consideration to linear equations, the change in time t of positions $\mathbf{x}^* = (x_1^*, x_2^*, x_3^*)$ and velocities $\mathbf{U}^* = (U_1^*, U_2^*, U_3^*)$, which are seen as properties of a fluid particle moving with the flow, may be written as ($i = 1, 2, 3$)

$$\frac{\mathrm{d}}{\mathrm{d}t} x_i^*(t) = U_i^*(t), \tag{1a}$$

$$\frac{\mathrm{d}}{\mathrm{d}t} U_i^*(t) = a_i + G_{ij}(U_j^* - \langle U_j \rangle) + G_i(\Theta^* - \langle \Theta_E \rangle) + b_{ij}\frac{\mathrm{d}W_j}{\mathrm{d}t}, \tag{1b}$$

where summation over repeated subscripts is assumed. Deterministic changes of the particle velocity are described through the first three terms on the right-hand side of Eq. (1b) with the unknown coefficients a_i, G_{ij}, G_i. These changes are the consequence of: gradients of mean Eulerian fields that are imposed by the boundary conditions (the first term), differences between the actual particle velocity and the Reynolds-averaged Eulerian velocity $\langle U \rangle$ (the second term) and between the actual potential particle temperature Θ^* and the Reynolds-averaged Eulerian potential temperature $\langle \Theta \rangle$ (the third term). Eulerian quantities are written without star in contrast to Lagrangian quantities. Their position dependence is replaced in the Lagrangian equations by the actual particle position. The last term describes the influence of a stochastic force (proportional to b_{ij} which has to be determined) that describes random accelerations due to the turbulent motions at the smallest scales. This term is characterized by the white noise $\mathrm{d}W_j/\mathrm{d}t$, which is a Gaussian process with vanishing mean values, $\langle \mathrm{d}W_j/\mathrm{d}t \rangle = 0$, and with uncorrelated values at different times, $\langle \mathrm{d}W_i/\mathrm{d}t\,(t) \cdot \mathrm{d}W_j/\mathrm{d}t'\,(t') \rangle = \delta_{ij}\,\delta(t - t')$. The symbol δ_{ij} is the Kronecker delta and $\delta(t - t')$ the delta function.

In a formal analogy to the velocity equation (1b), a stochastic equation for the potential temperature Θ^* is assumed, which is coupled to the particle motion, i.e.

$$\frac{\mathrm{d}}{\mathrm{d}t}\Theta^*(t) = a_\theta + G_{\theta j}(U_j^* - \langle U_j \rangle) + G_\theta(\Theta^* - \langle \Theta \rangle) + b_\theta \frac{\mathrm{d}W}{\mathrm{d}t}, \tag{2}$$

where the a_θ, $G_{\theta j}$, G_θ and b_θ have to be determined and $\mathrm{d}W/\mathrm{d}t$ has properties that correspond to those of $\mathrm{d}W_j/\mathrm{d}t$ in the velocity equation: $\langle \mathrm{d}W/\mathrm{d}t \rangle = 0$, $\langle \mathrm{d}W/\mathrm{d}t\,(t) \cdot \mathrm{d}W/\mathrm{d}t'\,(t') \rangle = \delta(t - t')$. Moreover, $\mathrm{d}W/\mathrm{d}t$ and $\mathrm{d}W_j/\mathrm{d}t$ are assumed to be uncorrelated over time steps that are much larger than the Kolmogorov microscale, $\langle \mathrm{d}W/\mathrm{d}t\,(t) \cdot \mathrm{d}W_j/\mathrm{d}t'\,(t') \rangle = 0$, so that the stochastic terms in the velocity and temperature equation do not cause systematic effects on the particle motion.

The Eqs. (1a) and (1b) and (2) can be transformed into a Fokker–Planck equation for the one-point joint velocity–temperature PDF of the flow (Gardiner, 1983; Risken, 1984). From that equation, transport equations can be derived for all the moments of this PDF by multiplication with the corresponding variables and integration. By invoking the incompressibility constraint $\partial U_k/\partial x_k = 0$, these equations read for the mean values

$$\frac{\partial \langle U_i \rangle}{\mathrm{d}t} + \langle U_j \rangle \frac{\partial \langle U_i \rangle}{\partial x_j} + \frac{\partial \langle u_i\, u_j \rangle}{\partial x_j} = a_i, \tag{3a}$$

$$\frac{\partial \langle \Theta \rangle}{\partial t} + \langle U_j \rangle \frac{\partial \langle \Theta \rangle}{\partial x_j} + \frac{\partial \langle u_j\, \theta \rangle}{\partial x_j} = a_\theta \tag{3b}$$

where $u_k = U_k - \langle U_k \rangle$ and $\theta = \Theta - \langle \Theta \rangle$ denote Eulerian fluctuations, i.e. $\langle u_i u_j \rangle$ and $\langle u_i \theta \rangle$ are the variances and covariances of the Eulerian velocity–temperature fields.

In the same way, budget equations for the variances of the velocity and potential temperature fields can be derived from the Eqs. (1a) and (1b) and (2). This leads to

$$\frac{\partial \langle u_i u_j \rangle}{\partial t} + \langle U_k \rangle \frac{\partial \langle u_i u_j \rangle}{\partial x_k} + \frac{\partial \langle u_k u_i u_j \rangle}{\partial x_k} + \langle u_k u_i \rangle \frac{\partial \langle U_j \rangle}{\partial x_k} + \langle u_k u_j \rangle \frac{\partial \langle U_i \rangle}{\partial x_k} = G_{ik} \langle u_k u_j \rangle + G_{jk} \langle u_k u_i \rangle + G_i \langle u_j \theta \rangle + G_j \langle u_i \theta \rangle + (b^2)_{ij}, \quad (4a)$$

$$\frac{\partial \langle u_i \theta \rangle}{\partial t} + \langle U_k \rangle \frac{\partial \langle u_i \theta \rangle}{\partial x_k} + \frac{\partial \langle u_k u_i \theta \rangle}{\partial x_k} + \langle u_k u_i \rangle \frac{\partial \langle \Theta \rangle}{\partial x_k} + \langle u_k \theta \rangle \frac{\partial \langle U_i \rangle}{\partial x_k} = G_{ij} \langle u_j \theta \rangle + G_i \langle \theta^2 \rangle + G_{0k} \langle u_k u_i \rangle + G_\theta \langle u_i \theta \rangle, \quad (4b)$$

$$\frac{\partial \langle \theta^2 \rangle}{\partial t} + \langle U_k \rangle \frac{\partial \langle \theta^2 \rangle}{\partial x_k} + \frac{\partial \langle u_k \theta^2 \rangle}{\partial x_k} + 2 \langle u_k \theta \rangle \frac{\partial \langle \Theta \rangle}{\partial x_k} = 2 G_{\theta i} \langle u_i \theta \rangle + 2 G_\theta \langle \theta^2 \rangle + b_\theta^2. \quad (4c)$$

Eqs. (3a) and (3b) and (4a)–(4c) contain the unknown coefficients a_i, a_θ and G_{ij}, G_i, $G_{\theta j}$, G_θ, b_{ij}, b_θ that appear on their right-hand sides. These quantities will be estimated in the next subsection through the comparison of Eqs. (3a) and (3b) and (4a)–(4c) with transport equations that are used in the second-order closure theory.

2.2. Estimation of coefficients

By invoking the Boussinesq approximation and the incompressibility constraint, Eqs. (3a) and (3b) are found to be consistent with the Eulerian transport equations for the mean momentum and potential temperature if

$$a_i = \nu \frac{\partial^2 \langle U_i \rangle}{\partial x_k \partial x_k} - \rho^{-1} \frac{\partial p}{\partial x_i} - g \delta_{i3},$$

$$a_\theta = \alpha \frac{\partial^2 \langle \Theta \rangle}{\partial x_k \partial x_k}. \quad (5)$$

Here, p is the Reynolds-averaged pressure, ρ the averaged fluid density, ν the kinematic viscosity, α the coefficient of molecular heat transfer and g the acceleration due to gravity. Molecular effects can be neglected for the problem considered here, therefore we find $a_\theta = 0$ according to relation (5). A corresponding direct conclusion with respect to a_i cannot be drawn due to the appearance of the pressure gradient and gravity acceleration.

The comparison of Eqs. (4a)–(4c) with the corresponding exact Eulerian RANS transport equations reveals that the terms on the right-hand side of Eqs. (4a)–(4c) correspond to parametrizations of the dissipation and pressure-strain terms. We now apply $(b^2)_{ij} = C_0 q^2/(2\tau)\, \delta_{ij}$ and $b_\theta^2 = C_1 \cdot \langle \theta^2 \rangle/(2\tau)$ for the coefficients of the stochastic forces in (1b) and (2) (van Dop et al., 1985; Thomson, 1987) with $C_0 = (k_1 - 2)/3$ and $C_1 = 2k_3 - 2k_4 - k_1$, and

$$G_{ij} = -\frac{k_t}{4\tau} \delta_{ij}, \quad G_i = \beta g \delta_{i3}, \quad G_{\theta i} = 0,$$

$$G_\theta = -\frac{2k_3 - k_1}{4\tau} \quad (6)$$

for the other coefficients. Here, the dissipation time scale $\tau = q^2/(2\varepsilon)$ is used with $q^2 = \langle u_i u_i \rangle$ as twice the TKE, and ε is the mean dissipation rate of TKE. Further, β is the thermal expansion coefficient, and k_1, k_3 and k_4 are closure parameters, see Section 4 for their estimation. The choice of G_{ij}, G_i, $G_{\theta j}$, G_θ, b_{ij}, b_θ corresponds to closure assumptions for the dissipation and pressure-strain terms according to Kolmogorov's (1942) theory and Rotta's (1951) hypothesis of a return-to-isotropy pressure-redistribution. There exist also other (more complicated) choices for the coefficients G_{ij}, G_i, $G_{\theta j}$, G_θ which satisfy the same parametrizations. This problem and the estimation of C_θ and C_1 are discussed elsewhere (Heinz, 1997). The Lagrangian equations (1a) and (1b) and (2) can also be constructed in consistency with more complex pressure-strain models (Craft et al., 1996), but the good performance of the applied models (see Sections 4 and 5) justifies the simple choice presented here.

2.3. Scaling of the Lagrangian equations

Lagrangian equations (1a) and (1b) and (2) describe the turbulent flow in dependence of the dissipation time scale τ that has to be provided. This quantity scales the dynamics and intensity of turbulent mixing processes, for instance, between a (buoyant) plume and the ambient flow, as illustrated in Fig. 1. The mixing processes may vary strongly with shear and stratification, so that τ has to be estimated in dependence on these quantities.

This can be achieved by postulating a budget equation for τ that completes the Lagrangian equations. All the details about the derivation of this relation, comparisons with other theories (which are used, e.g., to complete Eulerian turbulence models) and results of LES, DNS and measurements can be found in Heinz (1998a). This equation for τ may be written as

$$\frac{\mathrm{d}}{\mathrm{d}t} \tau = (C_{\varepsilon 2} - 1) - (C_{\varepsilon 1} - 1) \frac{2\tau}{q^2} \left\{ - \langle u_k u_l \rangle \frac{\partial \langle U_l \rangle}{\partial x_k} + \beta g \langle u_3 \theta \rangle \right\}, \quad (7)$$

where $C_{\varepsilon 1}$ and $C_{\varepsilon 2}$ are constants with standard values $C_{\varepsilon 1} = 1.56$ and $C_{\varepsilon 2} = 1.9$. The first term on the right-hand side of (7) causes a linear increase of τ in correspondence with Kolmogorov's (1942) frequency equation. This term is related to the dissipation of the plume-generated turbulence, which governs the initial stage of plume rise and plume rise in a calm ambient flow. It will be shown in Section 4.1 that the similarity laws of buoyant plume rise to production of turbulence (the terms in the bracket represent the production of TKE). This term brings the influence of the ambient turbulence into play, and, in particular, it explains the dependence of τ on shear and stratification. In accord with the Lagrangian equations (1a) and (b) and (2), the model (7) describes turbulent mixing processes with frequencies that are smaller than those related to the Kolmogorov microscale. These processes are induced by the initial plume buoyancy and forcing of the ambient flow, i.e. shear and stratification.

Eqs. (1a) and (1b) and (2) together with the expressions (5) and (6) represent in conjunction with the time scale Eq. (7) an LTM. According to these equations, the change of particle properties depends on the Eulerian mean velocities, temperatures, the covariances of these fields and the mean pressure gradient that is required for the calculation of a_i. These quantities can be derived from spatially averaged particle properties, as described by Pope (1985, 1995). Thus, these equations are closed for given boundary conditions and initial values for the positions, velocities and temperatures of particles.

3. Buoyant plume rise equations

Now, we use LTM (1a) and (1b), (2), (7) to derive the buoyant plume rise model. With reference to the constraints considered in Section 1 we apply some approximations, so that the procedures to calculate means, variances and the mean pressure gradient do not have to be applied. We consider a horizontally homogeneous turbulent flow with a vanishing Eulerian mean vertical velocity, $\langle U_3 \rangle = 0$, and a horizontal velocity along the x_1-axis, i.e. $\langle U_2 \rangle = 0$. The turbulence is driven by vertical gradients of the mean horizontal velocity $\langle U_1 \rangle$ and the mean potential temperature $\langle \Theta \rangle$, which are imposed through the boundary conditions. These assumptions correspond to a simple model for the atmospheric boundary layer above flat terrain.

Next, we consider the release of buoyant particles from a source localized in that flow. The buoyancy will mainly affect the vertical structure of the turbulence, so that we can assume that the mean flow field can be described again by the vertical characteristics of $\langle U_1 \rangle$ and $\langle \Theta \rangle$. The mean Eulerian vertical velocity that appears in Eq. (1b) has to be calculated as superposition of the mean vertical velocity of buoyant particles and the mean vertical velocity of the surrounding fluid. The resulting mean flow velocity can be expected to be small, because the upward motion of buoyant particles is compensated locally through downward motions of the surrounding fluid. In any case, neglecting the small mean Eulerian vertical velocity does not have any influence on the plume width, and could modify only somewhat the calculated mean plume height, but this quantity is found in agreement with LES data and measurements, see below. In addition to $\langle U_3 \rangle = 0$ we assume that spatial variations of $S = \partial \langle U_1 \rangle / \partial x_3$ and $N^2 = \beta g \, \partial \langle \Theta \rangle / \partial x_3$ (N is the Brunt–Väisälä frequency for a stable stratification) are small over the range of plume rise, so that a linear interpolation of their variations appears to be justified. Zhang and Ghoniem (1994a) also considered a constant N^2 in their LES of buoyant plume rise in stably stratified flow, see Section 4.2.

By invoking these assumptions, $\partial \langle U_1 \rangle / \partial x_k = S \, \delta x_{k3}$, $\langle U_2 \rangle = \langle U_3 \rangle = 0$, $\beta g \, \partial \langle \Theta \rangle / \partial x_k = N^2 \, \delta_{k3}$, where N^2 and S are constant, we see by means of Eqs. (4a)–(4c) that spatial variations of the variances may only arise from the gradients of triple correlations or the convective terms $\langle U_1 \rangle \partial \langle u_i u_j \rangle / \partial x_1$, $\langle U_1 \rangle \partial \langle u_i \theta \rangle / \partial x_1$, $\langle U_1 \rangle \partial \langle \theta^2 \rangle / \partial x_1$. In the first stage of buoyant plume rise, the plume turbulence is mainly determined by dissipation (see Section 4.1). This means that $\langle u_i u_j \rangle$, $\langle u_i \theta \rangle$ and $\langle \theta^2 \rangle$ change according to the terms on the right-hand side of Eqs. (4a)–(4c), so that the triple correlation and convective terms do not contribute significantly. At larger distances, the influence of ambient turbulence may lead to a levelling-off of the plume, which is induced by the terms related to shear and stratification on the left-hand sides of Eqs. (4a)–(4c). It may be expected that the contribution of horizontal gradients and triple correlation gradients to the description of the asymptotic stage of plume rise is also negligible, provided that no convective conditions are considered where the triple correlations are essential. Thus, it is justified to neglect these terms in Eqs. (4a)–(4c), which leads to the conclusion that the gradients of variances in Eq. (1b) disappear, i.e. in particular, $a_3 = 0$. These assumptions will be justified by the results presented below.

The Lagrangian equations read with these assumptions

$$\frac{\mathrm{d}}{\mathrm{d}t} x_3^* = U_3^*, \tag{8a}$$

$$\frac{\mathrm{d}}{\mathrm{d}t} U_3^* = -\frac{k_1}{4\tau} U_3^* + B^* + \sqrt{\frac{C_\theta \, q^2}{2\tau}} \frac{\mathrm{d}W_3}{\mathrm{d}t}, \tag{8b}$$

$$\frac{\mathrm{d}}{\mathrm{d}t} B^* = -\frac{2k_3 - k_1}{4\tau} B^* - N^2 \, U_3^* + \sqrt{\frac{C_1 \, (\beta g)^2 \, \langle \theta^2 \rangle}{2\tau}} \frac{\mathrm{d}W}{\mathrm{d}t}, \tag{8c}$$

where the influence of buoyancy on the particle motion (the second term on the right-hand side of Eq. (8b)) is written as $B^* = \beta g\ (\Theta^* - \langle\Theta\rangle)$ that gives the particle buoyancy acceleration. Eq. (8c) for B^* can be obtained from the temperature Eq. (2).

For the time scale Eq. (7) we obtain now

$$\frac{\mathrm{d}}{\mathrm{d}t}\tau = (C_{\varepsilon 2} - 1 - (C_{\varepsilon 1} - 1)\frac{2\tau}{q^2} \{ - S\langle u_1 u_3\rangle + \beta g\langle u_3\theta\rangle\}, \tag{9}$$

and the variances that are needed for the calculation of τ and the coefficients of the stochastic terms in (8b) and (8c) can be found as solutions of the equation system

$$\frac{\mathrm{d}}{\mathrm{d}t}\begin{pmatrix}\langle u_1 u_3\rangle\\ \langle u_1\theta\rangle\\ \langle u_3\theta\rangle\\ \langle u_3^2\rangle\\ \langle\theta^2\rangle\\ q^2\end{pmatrix} = \begin{pmatrix} -k_1/(2\tau) & \beta g & 0 & -S & 0 & 0\\ -N^2/\beta g & -k_3/(2\tau) & -S & 0 & 0 & 0\\ 0 & 0 & -k_3/(2\tau) & -N^2/\beta g & \beta g & 0\\ 0 & 0 & 2\beta g & -k_1/(2\tau) & 0 & (k_1-2)/(6\tau)\\ 0 & 0 & -2N^2/\beta g & 0 & -k_4/\tau & 0\\ -2S & 0 & 2\beta g & 0 & 0 & -1/\tau \end{pmatrix}\begin{pmatrix}\langle u_1 u_3\rangle\\ \langle u_1\theta\rangle\\ \langle u_3\theta\rangle\\ \langle u_3^2\rangle\\ \langle\theta^2\rangle\\ q^2\end{pmatrix}. \tag{10}$$

These Eqs. (8a)–(8c), (9) and (10) represent our buoyant plume rise model (BPRM). It is worth emphasizing that this model is obtained from the LTM (1a) and (1b), (2), (7) by neglecting a few terms of minor relevance, i.e. no additional parameters are introduced. The applied assumptions remove the problem to estimate mean velocities and temperatures and the mean pressure gradient by means of the procedure described in Section 2.3 (the equations appear in a closed form), and they permit the derivation of the plume rise scaling laws, see Section 4.1. The BPRM satisfies the demands on models for practical plume rise calculations as considered in Section 1, (i) it is computationally not expensive (the ordinary and stochastic differential equations can be solved easily), (ii) it can be applied to both stages of the buoyant plume rise and ambient conditions with varying shear and stratification, and (iii) it provides the plume statistics. Due to the neglect of the gradients of triple correlations, the BPRM does not reflect the typical features of convective flows (see, for instance, Willis and Deardorff, 1987; Luhar and Britter, 1992; Hurley and Physick, 1993; Weil et al., 1997), so that calculations of buoyant plume rise in such flows require the application of LTM.

4. Comparison with similarity theory and LES

First, the BPRM predictions will be compared with results of other theories and computational techniques, which can be done for uniform flows. In Section 4.1, we derive for a neutrally stratified flow the asymptotic features of the BPRM and compare these findings with the consequences of similarity theory. In Section 4.2, our calculations of buoyant plume rise in flow with varying stability are compared to LES data. The consideration of these limit cases of the BPRM at large and small times provides also information about the model parameters.

4.1. Similarity laws

For a neutrally stratified and uniform flow ($N = S = 0$), the time scale of turbulence τ at large times has to be independent of initial values. By neglecting the influence of the initial values of the time scale τ, vertical heat flux $\langle u_3\theta\rangle$ and temperature variance $\langle\theta^2\rangle$ on τ at $t \to \infty$, we find by means of Eqs. (9) and (10)

$$\tau = (C_{\varepsilon 2} - 1)\ t \tag{11}$$

as result of the first term on the right-hand side of Eq. (9), which corresponds with the consequences of similarity theory and permits the analytical calculation of the plume properties. By averaging Eqs. (8a)–(8c) and applying the initial values $\langle x_3^*\rangle = \langle U_3^*\rangle = 0$, $\langle B^*\rangle = \langle B_0\rangle$, we obtain for the mean plume height $\langle x_3^*\rangle$ for $t \to \infty$

$$\langle x_3^*\rangle = \frac{\langle B_0\rangle\,\tau_0^2}{m_1\,(m_1 - m_2)\,(C_{\varepsilon 2} - 1)^{2-m_1}}\ t_*^{m_i}, \tag{12}$$

where $t_* = t/\tau_0$ is the time normalized to the initial time scale τ_0. Additionally, the abbreviations $m_1 = 2 - (2k_3 - k_1)/(4\,[C_{\varepsilon 2} - 1)])$ and $m_2 = 1 - k_1/(4\,[C_{\varepsilon 2} - 1)])$ are used, and $m_2 < m_1$ is assumed as usually given with standard values for these parameters. The latter condition is required in order to estimate the leading power of t_* for the estimation of the asymptotic plume rise.

A corresponding result can also be obtained in the Eulerian approach (Weil, 1988; Netterville, 1990), where

$$\langle x_3^*\rangle = \left(\frac{3}{2\pi\beta_P^2}\right)^{1/3}\langle B_0\rangle\,\tau_0^2\,t_*^{2/3} \tag{13}$$

is derived with β_P as entrainment constant. We see that the results of the BPRM coincide with (13) when $m_1 = 2/3$, i.e.

$$C_{\varepsilon 2} = 1 + \frac{3k_1}{8}\left(\frac{k_3}{k_1} - \frac{1}{2}\right), \tag{14}$$

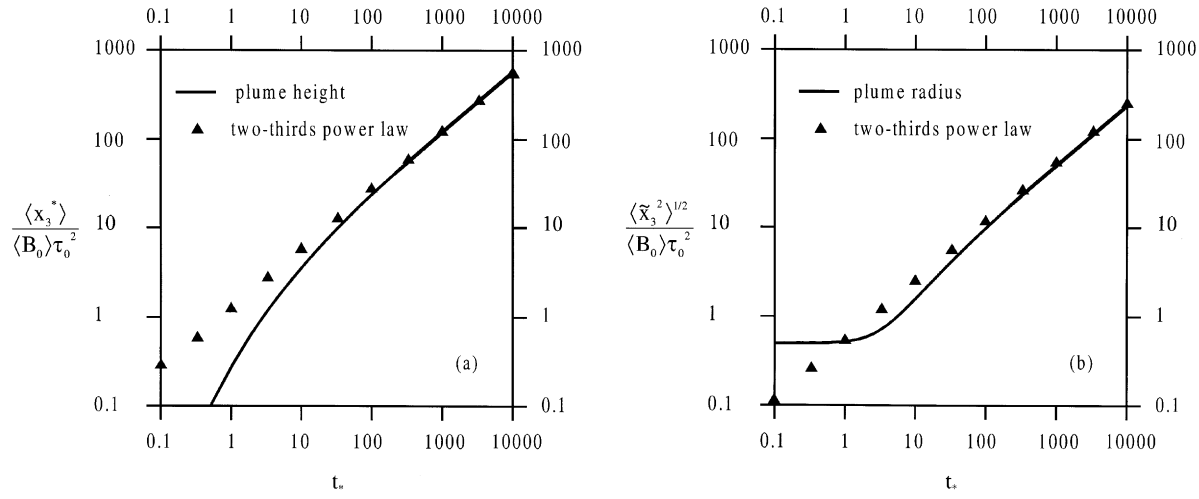

Fig. 3. The (a) normalized mean particle height and (b) square root of the mean particle dispersion as function of time calculated from the BPRM for a neutrally stratified and uniform flow (solid line). The triangles give the two–thirds power law that is predicted by the similarity theory.

and, when the factors of $t_*^{2/3}$ in Eqs. (12) and (13) are the same, which may be written as a condition for k_1 as

$$k_1 = 4\left(\frac{3\pi\beta_P^2}{2}\right)^{1/4}\left(\frac{k_3}{k_1}-\frac{1}{2}\right)^{-1/4}\left[1-\frac{1}{2}\left(\frac{k_3}{k_1}-\frac{1}{2}\right)\right]^{-3/4}. \tag{15}$$

Analytical expressions for the variances of the particle position, velocity and buoyancy $\langle\tilde{x}_3^2\rangle, \langle\tilde{U}_3^2\rangle, \langle\tilde{B}^2\rangle$ can be derived by integrating Eq. (10) in order to calculate q^2 and $\langle\theta^2\rangle$. For the comparison of these results with the consequences of the similarity theory, is most suited to consider $\langle\tilde{B}^2\rangle$, because only one power of t_* appears,

$$\langle\tilde{B}^2\rangle = \langle\tilde{B}_0^2\rangle\,[(C_{\varepsilon 2}-1)\,t_*] - k_4/(C_{\varepsilon 2-1}), \tag{16}$$

where $\langle\tilde{B}_0^2\rangle$ denotes the initial particle buoyancy variance. Similarity theory provides for the scaling law of the plume buoyancy variance $\langle\tilde{B}^2\rangle \sim t_*^{-8/3}$, but experimental evidence is lacking (Csanady, 1973). We see that the similarity theory constraint is satisfied, when

$$C_{\varepsilon 2} = 1 + \tfrac{3}{8}\ k_4. \tag{17}$$

This is an important result because it means that the coefficient of the stochastic force in the temperature equation has to vanish, i.e. $C_1 = 0$. This can be seen by combining Eqs. (14) and (17), which leads to the condition $2k_3 - k_1 = 2k_4$. By applying $C_1 = 0$, one finds asymptotically for the other variances

$$\langle\tilde{U}_3^2\rangle = \frac{\langle\tilde{B}_0^2\rangle}{\langle B\rangle_0^2}\langle U_3\rangle^2, \tag{18}$$

$$\langle\tilde{x}_3^2\rangle = \frac{\langle\tilde{B}_0^2\rangle}{\langle B\rangle_0^2}\langle x_3\rangle^2, \tag{19}$$

where $\langle U_3\rangle = \langle B_0\rangle\ \tau_0\ (C_{\varepsilon 2}-1)^{m_1-2}\, t_*^{m_1-1}/(m_1-m_2)$ can be found in the same way as the expression (12) for $\langle x_3\rangle$. By invoking relation (17), expressions (18) and (19) provide the correct similarity behaviours for these variances: $\langle\tilde{U}_3^2\rangle \sim t_*^{-2/3}$ and $\langle\tilde{x}_3^2\rangle \sim t_*^{4/3}$. With respect to relation (19) it is interesting to note that a corresponding assumption is applied in the Eulerian theory (Netterville, 1990), where the "active plume" radius is assumed to be proportional to the mean plume height over the source for $t_* \to \infty$.

Hence, the asymptotic features of the BPRM are found to be in agreement with the consequences of similarity theory provided that the stochastic source term in the particle buoyancy equation (the last term on the right-hand side of Eq. (8c)) is neglected and the parameters of the BPRM satisfy the consistency constraint (14). The computation of the normalized mean plume height $\langle x_3^*\rangle/(\langle B_0\rangle\tau_0^2)$ and radius $\langle\tilde{x}_3^2\rangle^{1/2}/(\langle B_0\rangle\tau_0^2)$ for these conditions is presented in Fig. 3, which shows how these curves approach asymptotically to their scaling laws. Details of the numerical calculation are given in Section 4.2 in conjunction with the description of the choice of parameters.

4.2. Stably stratified flow

Now, we investigate the effect of stability on buoyant plume rise by considering variations of the buoyancy parameter $B = 1/(N^2\,\tau_0^2)$, which is infinity in the calculations presented in the previous section. For small times, these estimates can be compared with the LES of Zhang and Ghoniem (1994a), provided that τ_0^2 is interpreted as $\tau_0^2 = \pi^{1/2}\,R_0/\langle B_0\rangle$, where R_0 is the radius of the active plume.

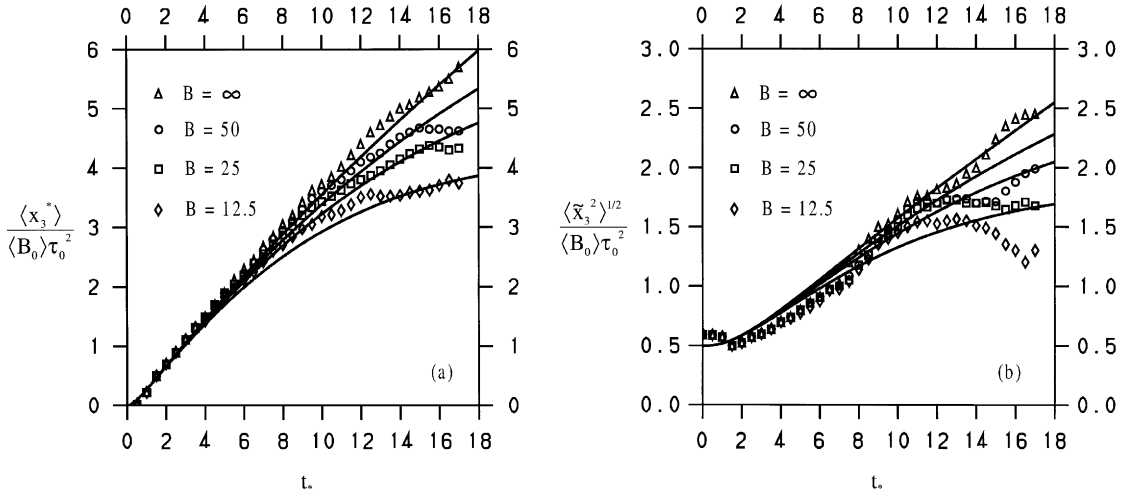

Fig. 4. The (a) normalized mean particle height and (b) square root of the mean particle dispersion as function of time calculated from the BPRM for different stabilities (solid lines). The symbols give the corresponding LES results of Zhang and Ghoniem (1994a) for various values of the buoyancy parameter B.

In Fig. 4a, our calculated normalized plume height $\langle x_3^* \rangle / (\langle B_0 \rangle \tau_0^2)$ is compared to these LES data (our notation $\langle x_3^* \rangle / (\langle B_0 \rangle \tau_0^2)$ and t_* corresponds to z and x in the notation of Zhang and Ghoniem, respectively). We see that the agreement between the results obtained in both approaches is very good. For $B = \infty$, our curve coincides with the curve presented in Fig. 3a, which approaches asymptotically to the two-thirds power law. In Fig. 4b, our calculation of $\langle \tilde{x}_3^2 \rangle^{1/2} / (\langle B_0 \rangle \tau_0^2)$ is compared to the vertical plume radius that is provided by LES. The latter quantity is the half plume width, which is "defined in terms of the maximum vertical extension of the plume cross section, along the downwind distance", see Zhang and Ghoniem (1994a). Although the plume radius is not identically defined in both approaches, we see that the effect of stability is reflected very similar.

These calculations are performed with 25 000 particles and a time step $\Delta t = 0.05\, \tau_0$ by applying a Runge–Kutta procedure. For the initial values of particle properties we used: $x_3^* = 0.5 \langle B_0 \rangle \tau_0^2 \quad \xi_1, \quad U_3^* = 0$ and $B^* = \langle B_0 \rangle [1 + \langle \tilde{B}_0^2 \rangle^{1/2} / \langle B_0 \rangle \, \xi_2]$, where ξ_i ($i = 1, 2$) are Gaussian-distributed random processes with $\langle \xi_i \rangle = 0$, $\langle \xi_i^2 \rangle = 1$ and $\langle \xi_1 \xi_2 \rangle = 0$. The factor 0.5 of x_3^* was chosen in accord with the LES data, see Fig. 4b. The setting of $\langle \tilde{B}_0^2 \rangle^{1/2} / \langle B_0 \rangle$ for the estimation of B_0 is important for the asymptotic features of the variances, see Eqs. (16), (18) and (19). By means of relation (19) and the calculation of the ratio between the plume radius and height by the measurements presented in Section 5, we derived $\langle \tilde{B}_0^2 \rangle^{1/2} / \langle B_0 \rangle = 0.42$. The initial values for equation system (10) that are required in addition to $\langle u_3 \theta \rangle = \langle \theta^2 \rangle = 0$ are chosen as: $\langle u_1 u_3 \rangle = \langle u_3^2 \rangle = \langle u_1 \theta \rangle = 0$ and $q^2 = 0.1 \langle B_0 \rangle^2 \tau_0^2$. The choice of the latter value has only a minor influence on the plume radius at very small times. Three relations for the model parameters k_1, k_3, k_4, $C_{\varepsilon 1}$ and $C_{\varepsilon 2}$ are given through Eqs. (14), (15) and (17). $C_{\varepsilon 1}$ was related to $C_{\varepsilon 2}$ by $C_{\varepsilon 1} = 1 + (C_{\varepsilon 2} - 1)/1.6$ (Heinz, 1998a). To estimate the remaining open parameter, we estimated the effect of $C_{\varepsilon 2}$ on the variation of the mean plume height with the buoyancy parameter B, see Fig. 4a. We found that $C_{\varepsilon 2} = 1.286$ brought the best agreement between the BPRM and LES predictions. By adopting this value and $\beta_P = 0.49$ (Zhang and Ghoniem, 1994a), the other parameters are found as $k_1 = 9.18$, $k_3 = 4.99$ and $k_4 = 0.4$. The values for k_1 and k_3 are within the range of estimated variations of these quantities, but k_4 is found to be smaller than usually applied values (Heinz, 1998a). This parameter characterizes the ratio of the mean dissipation rate of the temperature variance to that of TKE, which can be expected to be small for the conditions considered where the turbulence dissipation dominates.

5. Comparison with plume rise measurements

Now we compare the predictions of the BPRM with results of measurements. The assessment of the influence of the ambient conditions requires simultaneous measurements of plume characteristics and wind shear and stability of the atmosphere. To our knowledge, these data sets are sparse. We compared our model predictions with lidar plume rise measurements, which have been analyzed by Erbrink (1994). These measurements were performed near power plant stacks at different sites in Holland, Germany and Poland in 1988–1990 for a wide

variety of (winter and summer) conditions. For that comparison, we used the plume rise measurements near the power stations Nijmegen, Amer, Buggenum and Lippendorf in Holland and Germany. We did not consider the lidar measurements in Cracow since these concerned a merged plume, which originated from two stacks with different heights (225 and 260 m) at a distance of 75 m.

The BPRM equations can be made dimensionless by combination with the corresponding powers of $\langle B_0 \rangle$ and τ_0. The calculated normalized plume heights $\langle x_3^* \rangle / (\langle B_0 \rangle \tau_0^2)$ and radius $\langle \tilde{x}_3^2 \rangle^{1/2} / (\langle B_0 \rangle \tau_0^2)$ depend then upon the normalized initial velocity $V_s/(\langle B_0 \rangle \tau_0)$, the shear number $S \tau_0$ and the buoyancy parameter $B = 1/(N^2 \tau_0^2)$. The influence of these quantities on plume rise is considered in the next three subsections.

5.1. Effect of exit velocity

In order to calculate $V_s/(\langle B_0 \rangle \tau_0)$, $S \tau_0$ and B, we have to derive the scaling quantities for the BPRM, $\langle B_0 \rangle$ and τ_0, from the emission data and meteorological conditions. The initial time scale is calculated by means of $\tau_0^2 = \pi^{1/2} R_0 / \langle B_0 \rangle$ as above, and the initial buoyancy by its relation to the initial plume buoyancy flux F_0 (Netterville, 1990), $\langle B_0 \rangle = F_0/(U_0 R_0^2)$. F_0 is then calculated by means of $F_0 = g R_s^2 V_s (T_s - T_a)/T_s$ (Seinfeld, 1986), and the initial radius R_0 of the active plume is obtained by $R_0 = R_s (2 V_s T_a)^{1/2}/(U_0 T_s)^{1/2}$ (Netterville, 1990). Here, U_0 is the mean horizontal velocity at stack height, R_s the stack radius, V_s the exit velocity of the emissions, and T_s and T_a are the temperatures of the emission and the surrounding flow at stack height, respectively. The estimation of τ_0 provides a range $1.7 \text{ s} < \tau_0 < 4.5 \text{ s}$, and the values for $\langle B_0 \rangle$ are found in a range $1.0 \text{ m s}^{-2} < \langle B_0 \rangle < 2.8 \text{ m s}^{-2}$.

By means of these estimates of $\langle B_0 \rangle$ and τ_0, we find the normalized initial velocity within a range $0 < V_s/(\langle B_0 \rangle \tau_0) < 5$ for all measured data. Fig. 5 shows the mean plume height (the plume radius is not influenced by variations of $V_s/(\langle B_0 \rangle \tau_0)$) for a neutrally stratified and uniform flow for the two limit cases $V_s/(\langle B_0 \rangle \tau_0) = 0$ and $V_s/(\langle B_0 \rangle \tau_0) = 5$. The calculation of $t_* = t/\tau_0$ for the measured data reveals that $t_* > 13.4$ in all cases. For that range of t_*, we find the effect of $V_s/(\langle B_0 \rangle \tau_0)$ to be negligible, in particular because most of the data have values $V_s/(\langle B_0 \rangle \tau_0)$ that are smaller than 5. Thus, as done before we can neglect $V_s/(\langle B_0 \rangle \tau_0)$ for our study of the effects of shear and stratification.

5.2. Effect of shear

Calculations of the normalized plume height $\langle x_3^* \rangle / (\langle B_0 \rangle \tau_0^2)$ and radius $\langle \tilde{x}_3^2 \rangle^{1/2} / (\langle B_0 \rangle \tau_0^2)$ are presented in the Fig. 6 for a neutrally stratified flow with different values of the dimensionless shear number $S \tau_0$. We see,

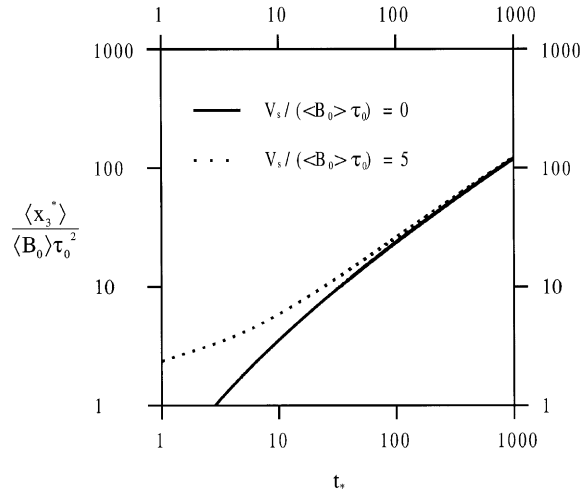

Fig. 5. The normalized mean particle height as function of time for a neutrally stratified and uniform flow in dependence on the normalized initial particle velocity $V_s/(\langle B_0 \rangle \tau_0)$.

the stronger the shear, the stronger is also the levelling-off of the plume height and radius since the difference of the temperatures of the plume and the ambient fluid vanishes faster due to the increase of the ambient turbulence intensity. Fig. 6 shows that there is no significant effect of shear for $t_* < 250$ for the considered values of $S \tau_0$. For virtually all measurements, t_* and $S \tau_0$ were smaller than 250 and 0.06, respectively. This fact leads to the conclusion that the atmospheric conditions for the plume rise measurements do not allow an assessment of the effect of shear.

Similar results for the effect of shear can also be obtained by Eulerian methods, as described by Djurfors and Netterville (1978). They assumed that the vertical profile of the mean horizontal wind can be described by a power law $\langle U_1 \rangle = U_0 (1 + x_3/z_0)^{\mu}$, where x_3 is the height above the stack, and z_0 a reference height. This velocity profile causes a modification of the two-thirds power law: $\langle x_3^* \rangle t^{2/(3+\mu)}$. Quantitative comparisons with their results are difficult. The power $\mu = [\partial \langle U_1 \rangle / \partial x_3]$ $(x_3 = 0)$ z_0/U_0 represents a dimensionless shear number as $S \tau_0$, but the time scales in these shear numbers are defined differently: $z_0/U_0 = (1 + \mu/2) R_s/(U_s \beta_P)$ whereas our model applies according to the LES data $\tau_0 = \pi^{1/4} R_0^{1/2}/\langle B_0 \rangle^{1/2}$, so that comparisons depend on the time scale ratio.

5.3. Effect of stability

Fig. 7a shows a scatter plot of measured plume heights, which are made dimensionless by dividing them by $\langle B_0 \rangle \tau_0^2$, versus the corresponding modelled normalized plume heights. The buoyancy parameter B varies in these

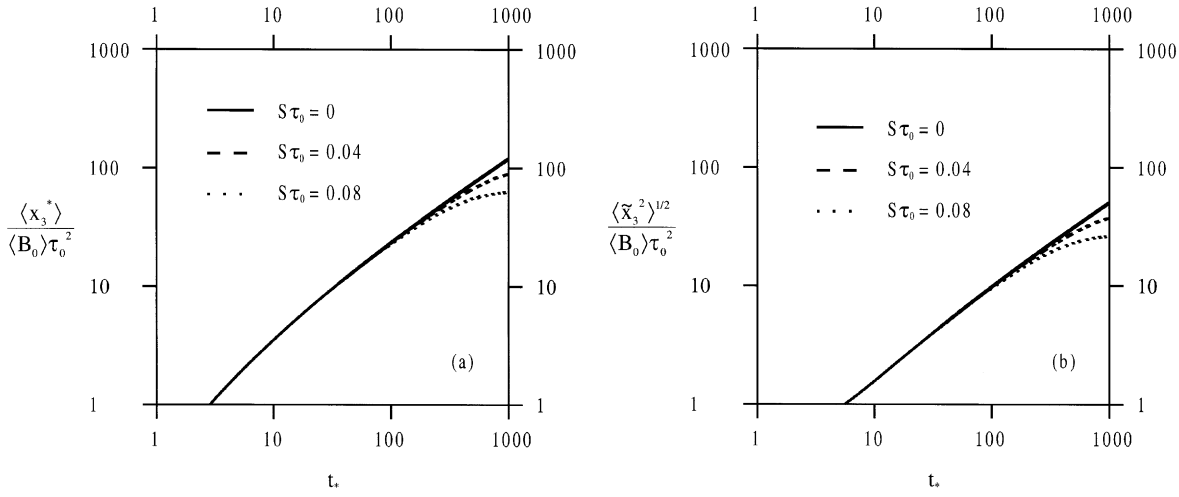

Fig. 6. The (a) normalized mean particle height and (b) square root of the mean particle dispersion as function of time for a neutrally stratified flow in dependence on the dimensionless shear number $S\ \tau_0$.

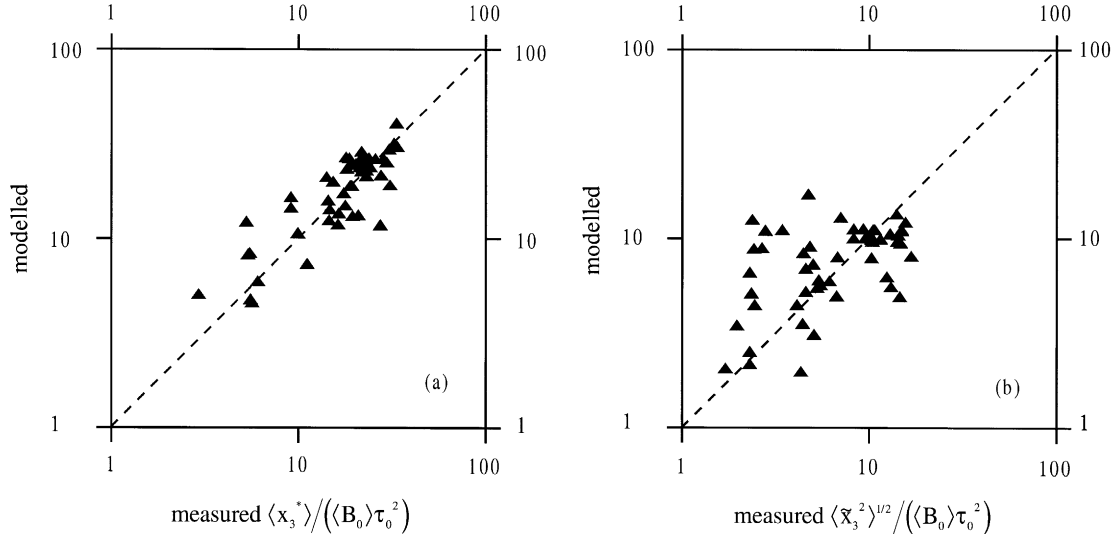

Fig. 7. Scatter plots of the measured versus modelled (a) normalized mean particle height and (b) square root of the mean particle dispersion. In the measurements, the buoyancy parameter B varies between 66 and infinity.

measurements between 66 and infinity, but in the most cases B is higher than 400. This figure reveals that the agreement between the observed plume heights and our predictions is very good. This means in particular that our model predictions are not only in accord with the two-thirds power law (see Fig. 3a), but estimate correctly the levelling-off of the plume due to stability, see Fig. 4a. Fig. 7b shows the same comparison in respect to the plume radius, which reveals also a good agreement. As can be expected, the scatter of data is larger here than for the plume heights. It is worth emphasizing that Fig. 7b demonstrates that the two-thirds scaling law for the plume radius provides a good guideline for the assessment of the plume spreading.

6. Summary and concluding remarks

We applied a new concept to calculate buoyant plume rise. In contrast to RANS or Lagrangian methods applied previously, the turbulent mixing between the plume and ambient flow is simulated for varying conditions

without having to make ad hoc assumptions on entrainment processes. The model input data are measurable and the computational costs of the BPRM are low compared to LES. The plume rise calculations presented in Section 5, e.g. can be performed in a few minutes on a PC. Thus, the BPRM is well-suited for routine applications.

We compared our model with the consequences of similarity theory, LES and measurements in the atmosphere. For emissions into a flow without shear and stratification, the similarity theory predictions are found as a special case of our theory. By choosing suitable relations between the model parameters and neglecting the source term for particle buoyancy fluctuations ($C_1 = 0$), our asymptotic plume rise predictions for the mean plume height and radius agree exactly with the similarity theory results. The condition $C_1 = 0$ represents an interesting theoretical result and rises the questions about the need to consider a stochastic source term in the particle temperature equation. The conclusion that can be drawn from the comparisons with measurements in the atmosphere and LES is that the contribution of this term is small for the conditions considered here, which is plausible because the buoyant plume rise is determined essentially by the dissipation of plume turbulence. However, we believe that the consideration of such a (small) source term could be important under more complex conditions, e.g. to explain the penetration of inversion layers or the plume spreading in the strongly stably stratified atmosphere. For emissions into flows with shear and stratification, the BPRM provides the typical levelling-off of plume height and radius. The effect of shear on plume rise is predicted in correspondence to results obtained in the Eulerian framework, and the effect of stability is predicted in a good agreement with LES data and measurements in the atmosphere.

Acknowledgements

Many thanks in particular to Dr. Hans Erbrink (KEMA Research Department, The Netherlands) who supported us with detailed information about the atmospheric plume rise measurements that were applied to assess our model. Many thanks also to the referees for their very helpful comments.

References

Anfossi, D., Ferrero, E., Brusasca, G., Marzorati, A., Tinarelli, G., 1993. A simple way of computing buoyant plume rise in Lagrangian stochastic dispersion models. Atmospheric Environment 27A, 1443–1451.

Briggs, G.A., 1975. Plume rise predictions. Lectures on Air Pollution and Environmental Impact Analyses. American Mathematical Society, Providence, RI, pp. 59–111.

Cogan, J.L., 1985. Monte Carlo dispersion of buoyant dispersion. Atmospheric Environment 19, 867–878.

Csanady, G.T., 1973. Turbulent Diffusion in the Environment. Geophysics and Astrophysics Monographs, vol. 3. R. Reidel, Dordrecht.

Craft, T.J., Ince, N.Z., Launder, B.E., 1996. Recent developments in second-moment closure for buoyancy-affected flows. Dynamics of Atmosphere and Oceans 23, 99–114.

Djurfors, S., Netterville, D., 1978. Buoyant plume rise in nonuniform wind conditions. Journal of the Air Pollution Control Association 28, 780–784.

Erbrink, H.J., 1994. Plume rise in different atmospheres: a practical scheme and some comparisons with LIDAR measurements. Atmospheric Environment 28, 3625–3636.

Fox, R.O., 1996. Computational methods for turbulent reacting flows in the chemical process industry. Revue de l'Institut Francais du Pétrole 51, 215–243.

Gangoiti, G., Sancho, J., Ibarra, G., Alonso, L., García, J.A., Navazo, M., Durana, N., Ilardia, J.L., 1997. Rise of moist plumes from tall stacks in turbulent and stratified atmospheres. Atmospheric Environment 31A, 253–269.

Gardiner, C.W., 1983. Handbook of Statistical Methods. Springer, Berlin.

Gonzales, M., 1997. Analysis of the effect of microscale turbulence on atmospheric chemical reactions by means of the P.D.F. approach. Atmospheric Environment 31, 575–586.

Heinz, S., 1997. Nonlinear Lagrangian equations for turbulent motion and buoyancy in inhomogeneous flows. Physics of Fluids 9, 703–716.

Heinz, S., 1998a. Time scales of stratified turbulent flows and relations between second–order closure parameters and flow numbers. Physics of Fluids 10, 958–973.

Heinz, S., 1998b. Connections between Lagrangian stochastic models and the closure theory of turbulence for stratified flows. International Journal of Heat and Fluid Flow 19, 193–200.

Hurley, P., Physick, W., 1993. Lagrangian particle modelling of buoyant point sources: plume rise and entrainment under convective conditions. Atmospheric Environment 27A, 1579–1584.

Kolmogorov, A.N., 1942. Equations of turbulent motion of an incompressible fluid. Izvestiya Academii Nauk SSSR, Seriya Fiziko 6, 56–58.

Luhar, A.K., Britter, R.E., 1992. Random-walk modelling of buoyant-plume dispersion in the convective boundary layer. Atmospheric Environment 26A, 1283–1298.

Netterville, D.D., 1990. Plume rise, entrainment and dispersion in turbulent winds. Atmospheric Environment 24A, 1061–1081.

Nieuwstadt, F.T.M., de Valk, J.P.J.M.M., 1987. A large eddy simulation of buoyant and non-buoyant plume dispersion in the atmospheric boundary layer. Atmospheric Environment 21, 2573–2587.

Nieuwstadt, F.T.M., 1992a. A large-eddy simulation of a line source in a convective atmospheric boundary laye—I. Dispersion characteristics. Atmospheric Environment 26A, 485–495.

Nieuwstadt, F.T.M., 1992b. A large-eddy simulation of a line source in a convective atmospheric boundary layer — II. Dynamics of a buoyant line source. Atmospheric Environment 26A, 497–503.

Pope, S.B., 1985. PDF Methods for turbulent reactive flows. Progress in Energy Combustion Science 11, 119–192.

Pope, S.B., 1994a. On the relationship between stochastic Lagrangian models of turbulence and second-moment closures. Physics of Fluids 6, 973–985.

Pope, S.B., 1994b. Lagrangian PDF methods for turbulent flows. Annual Review of Fluid Mechanics 26, 23–63.

Pope, S.B., 1995. Particle methods for turbulent flows: integration of stochastic model equations. Journal of Computational Physics 117, 332–349.

Risken, H., 1984. The Fokker-Planck Equation. Springer, Berlin.

Rodean, H.C., 1996. Stochastic Lagrangian models of turbulent dispersion. Meteorological monographs, vol. 26 (48). American Meteorological Society, Boston, USA.

Rotta, J.C., 1951. Statistische theorie nichthomogener turbulenz. Zeitschrift für Physik 129, 547–572.

Sawford, B.L., 1986. Generalized random forcing in random-walk turbulent dispersion models. Physics of Fluids 29, 3582–3585.

Sawford, B.L., 1993. Recent developments in the Lagrangian stochastic theory of turbulent dispersion. Boundary-Layer Meteorology 62, 197–215.

Seinfeld, J.H., 1986. Atmospheric Chemistry and Physics of the Air Pollution. Wiley, New York.

Thomson, D.J., 1987. Criteria for the selection of stochastic models of particle Trajektories in turbulent flows. Journal of Fluid Mechanics 180, 529–556.

van Dop, H., Nieuwstadt, F.T.M., Hunt, J.C.R., 1985. Random walk models for particle displacements in inhomogeneous unsteady turbulent flows. Physics of Fluids 28, 1639–1653.

van Dop, H., 1992. Buoyant plume rise in a Lagrangian framework. Atmospheric Environment 26A, 1335–1346.

Weil, J.C., 1988. Plume rise. In: Venkatram, A., Wyngaard, J.C. (Eds.), Lectures on Air Pollution Modeling. American Meteorological Society, Boston, pp. 119–166.

Weil, J.C., Corio, L.A., Brower, R.P., 1997. A PDF dispersion model for buoyant plumes in the convective boundary layer. Journal of Applied Meteorology 36, 982–1003.

Willis, G.E.., Deardorff, J.W., 1987. Buoyant plume dispersion and inversion entrapment in and above a laboratory mixed layer. Atmospheric Environment 21, 1725–1735.

Wilson, J.D., Sawford, B.L., 1996. Review of Lagrangian stochastic models for trajectories in the turbulent atmosphere. Boundary-Layer Meteorology 78, 191–210.

Zannetti, P., Al-Madani, N., 1984. Simulation of transformation, buoyancy and removal processes by Lagrangian particle methods. In: Wispelaere, Ch. (Ed.), Proceedings of the 14th International Technical Meeting Air Pollution Modelling and its Application, pp. 733–744.

Zhang, X., Ghoniem, A.F.A., 1993. Computational model for the rise and dispersion of wind–blown, buoyancy driven plumes–I. Neutrally stratified atmosphere. Atmospheric Environment 27A, 2295–2311.

Zhang, X., Ghoniem, A.F.A., 1994a. Computational model for the rise and dispersion of wind-blown, buoyancy driven plumes-II. Linearly stratified atmosphere. Atmospheric Environment 28, 3005–3018.

Zhang, X., Ghoniem, A.F.A., 1994b. Computational model for the rise and dispersion of wind-blown, buoyancy driven plumes—III. Penetration of atmospheric inversion. Atmospheric Environment 28, 3019–3032.